Corrosion Science 140 (2018) 223–230

Contents lists available at ScienceDirect

Corrosion Science

journal homepage: www.elsevier.com/locate/corsci

Nano-Ti_5Si_3 leading to enhancement of oxidation resistance

Y. Jiao[b], L.J. Huang[a,b,*], S.L. Wei[b], L. Geng[a,b], M.F. Qian[b], S. Yue[c]

[a] State Key Laboratory of Advanced Welding and Joining, Harbin Institute of Technology, Harbin, PR China
[b] School of Materials Science and Engineering, Harbin Institute of Technology, P.O. Box 433, Harbin 150001, PR China
[c] Department of Mining and Materials Engineering, McGill University, Montreal, Quebec, H3A 2B2, Canada

ARTICLE INFO

Keywords:
Titanium alloys
Titanium matrix composites
Nano-Ti_5Si_3
Oxidation behaviors
Anti-oxidation mechanisms

ABSTRACT

Nano-Ti_5Si_3 particles were formed via solution and precipitation, which drastically increased mechanical properties of (Ti_5Si_3 + TiBw)/Ti6Al4V composites. In the present work, compared with Ti6Al4V alloy at 700 and 800 °C, nano-Ti_5Si_3 particles led to remarkable enhancement of oxidation resistance, which increased with increasing Ti_5Si_3 fractions. The contributions of nano-Ti_5Si_3 particles were in two aspects: 1) were beneficial to forming dense and thin scale of mixed Al_2O_3 and SiO_2, which suppressed oxygen from permeating into matrix; 2) resulted in refinement of TiO_2 particles, which could enhance the toughness and relative density of oxide scale. The two-level hierarchical microstructure also stabilized oxide scale.

1. Introduction

The unique characteristics of high specific strength, low density and excellent corrosion resistance have made Titanium (Ti) alloys become candidate materials for aerospace, automotive, military and chemical applications [1,2]. However, the service temperature of Ti alloys is often restricted to below 600 °C, due to their strong oxidation propensity and low oxidation resistance [3]. When Ti alloys were exposed to oxygen atmosphere above 600 °C, non-protective oxide layer would form and serious surface spallation would occur [4]. Discontinuously reinforced titanium matrix composites (DRTMCs) have been extensively investigated to overcome such shortcomings, owing to their high temperature durability, high modulus as well as good oxidation and creep resistance [5–8]. However, traditional titanium matrix composites (TMCs) with a homogeneous structure had the defect of room-temperature brittleness, which seriously obstructs their practical applications [9]. Titanium matrix composites with a network structure have improved the plasticity and exhibited excellent mechanical properties at room and elevated temperatures [5].

TiB whiskers (TiBw) were regarded as appropriate reinforcement for reinforcing Ti alloys, on account of their high strength, good thermal and chemical compatibility with Ti [5,10]. However, TiBw reinforced Ti matrix composites showed lower oxidation resistance than Ti alloys at elevated temperatures. For example, Zhang et al. [11] presented that TiB reduces the oxidation resistance of Ti-6Al-1.2B alloy, due to the formation and evaporation of B_2O_3 at 750–900 °C. Hu et al. [6] reported that compared with the Ti60 alloy from 600 °C to 900 °C, the oxidation resistance of TiBw/Ti60 composites is decreased by TiBw reinforcements introducing more boundaries. Owing to good oxidation and creep resistance, Ti_5Si_3 has been widely studied as promising materials for high-temperature applications [12]. The Ti_5Si_3 particles could continuously release silicon into oxide layer, and improved oxidation resistance with increasing oxidation time [13]. The addition of Si was an effective method to improve oxidation resistance and oxide layer adherence of Ti alloys [14,15]. The formation of SiO_2 on the surface of Ti alloys was beneficial to increasing oxidation resistance [16]. The interactions of O-Ti atoms could be weakened by the segregation of Si on a TiAl surface [17]. However, when Si content exceeded 2 wt.%, the formation of coarse Ti_5Si_3 phase caused a rapid reduction of ductility [18], which could be improved by nano-scaled Ti_5Si_3 effectively [19]. In our previous work [20], the mechanical properties of (Ti_5Si_3 + TiBw)/Ti6Al4V composites were increased via nano-Ti_5Si_3 and the second-level network microstructure. As well as maintaining high mechanical properties, the introduction of fine Ti_5Si_3 reinforcement into the TiBw/Ti composites (through the effects of sintering pressure and the first-level network microstructure) is a promising way to enhance oxidation resistance.

In the present work, the oxidation behaviors of (Ti_5Si_3 + TiBw)/Ti6Al4V composites with hierarchical microstructure were systematically investigated at 700 and 800 °C in air. The fractions of Ti_5Si_3 and TiBw reinforcements were optimized to achieve enhanced oxidation resistance. Microstructure characteristics of composites and morphology of oxide scale were observed, in order to reveal the anti-oxidation mechanisms of (Ti_5Si_3 + TiBw)/Ti6Al4V composites. The present findings provide significant guidance for fabricating Ti alloys reinforced by nano-Ti_5Si_3 with high oxidation resistance.

* Corresponding author at: State Key Laboratory of Advanced Welding and Joining, Harbin Institute of Technology, Harbin, PR China.
E-mail address: huanglujun@hit.edu.cn (L.J. Huang).

https://doi.org/10.1016/j.corsci.2018.05.043
Received 1 March 2018; Received in revised form 28 May 2018; Accepted 31 May 2018
Available online 02 June 2018
0010-938X/

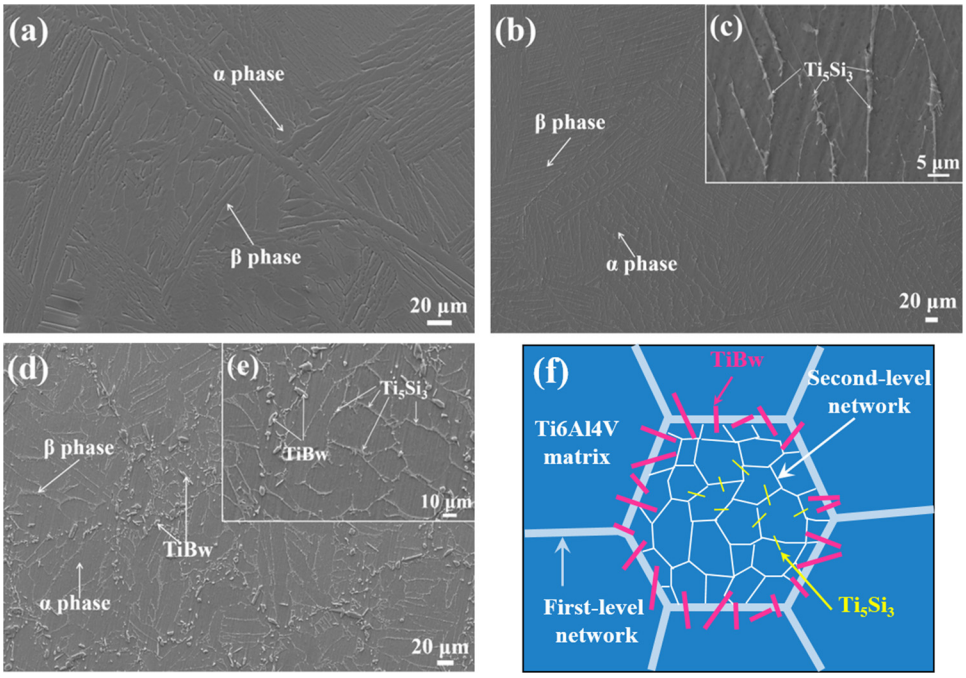

Fig. 1. SEM micrographs of as-sintered alloy and composites: (a) Ti6Al4V alloy, (b) and (c) 4 vol.%Ti_5Si_3/Ti6Al4V composite, (d) and (e) (4 vol.%Ti_5Si_3 + 3.4 vol.%TiBw)/Ti6Al4V composite, (f) a schematic illustration of the composite with a two-level network microstructure.

2. Experimental procedures

Based on our previous investigations [10,20,21], Ti6Al4V alloy (Fig. 1(a)), Ti_5Si_3/Ti6Al4V composite (Fig. 1(b) and (c)) and (Ti_5Si_3 + TiBw)/Ti6Al4V composite with a two-level network architecture (Fig. 1(d), (e) and (f)) were fabricated by low-energy milling and reaction hot pressing successfully. Ti_5Si_3 particles distribute within the β-Ti phases and forms a second-level network microstructure. TiB whiskers locate around the Ti6Al4V particles and generates a first-level network microstructure.

In this study, the as-sintered Ti6Al4V alloys, 4 vol.%Ti_5Si_3/Ti6Al4V composites and (Ti_5Si_3 + TiBw)/Ti6Al4V composites with different reinforcements fractions were used for oxidation tests at 700 and 800 °C, for a time period of 100 h. The dimension of samples subjected to oxidation was 8 × 8 × 3 [mm]. Prior to oxidation tests, the samples were prepared following standard metallographic techniques. Firstly, the samples were grinded by a series of abrasive papers. Afterwards, the samples were mechanically polished with Cr_2O_3 powder and etched in Kroll's solution (5% HF + 10% HNO_3 + 85% H_2O) for 8 s. Isothermal oxidation experiments were performed in a laboratory air circulated furnace. The specimens were weighed by an electronic balance with accuracy of 0.1 mg, before and after oxidation tests. The weight gain values of three samples were averaged for each oxidation condition. After oxidation tests, the oxidized specimens were cut transversely to reveal the cross-section of the oxidized surface, and mounted by conductive powder. Following mounting, the specimens were prepared using standard metallographic techniques to observe the cross-profile characteristics.

Phase compositions of oxide scale on oxidized specimens were carried out using X-Ray Diffraction (XRD; Empyrean) with Cu-K_α radiation. The surface morphology of specimens was characterized by a scanning electron microscope (SEM; ZEISS SUPRA 55 SAPPHIRE) equipped with energy dispersive X-ray spectroscope (EDS) and transmission electron microscope (TEM; FEI Talos F200x).

3. Results and discussion

3.1. Oxidation thermodynamics

When the (Ti_5Si_3 + TiBw)/Ti6Al4V composites are oxidized in air at 700 and 800 °C, there are four reactions can occur in the composites as follows.

$$Ti(s) + O_2(g) = R\text{-}TiO_2(s) \quad (1)$$

$$\frac{4}{3}Al(s) + O_2(g) = \frac{2}{3}Al_2O_3(s) \quad (2)$$

$$\frac{1}{8}Ti_5Si_3(s) + O_2(g) = \frac{5}{8}R\text{-}TiO_2(s) + \frac{3}{8}SiO_2(s) \quad (3)$$

$$\frac{4}{7}TiB(s) + O_2(g) = \frac{4}{7}R\text{-}TiO_2(s) + \frac{2}{7}B_2O_3 \quad (4)$$

(B_2O_3 : solid if T < 450 °C and liquid if T > 450 °C).

Fig. 2 shows the calculation results of Gibbs free energy change (ΔG) of the above-mentioned reactions using the data of Liang et al. [22]. It

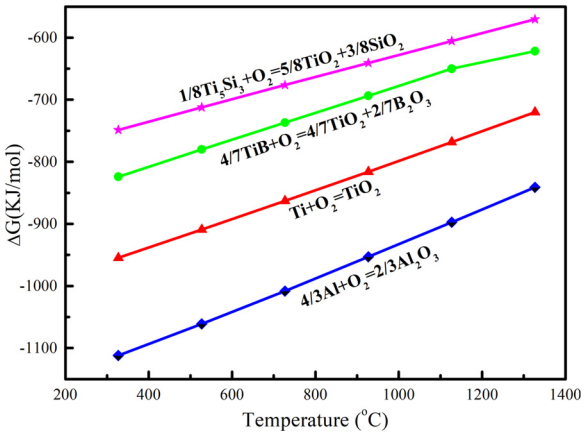

Fig. 2. The calculation results of Gibbs free energy (ΔG) for oxidation reactions.

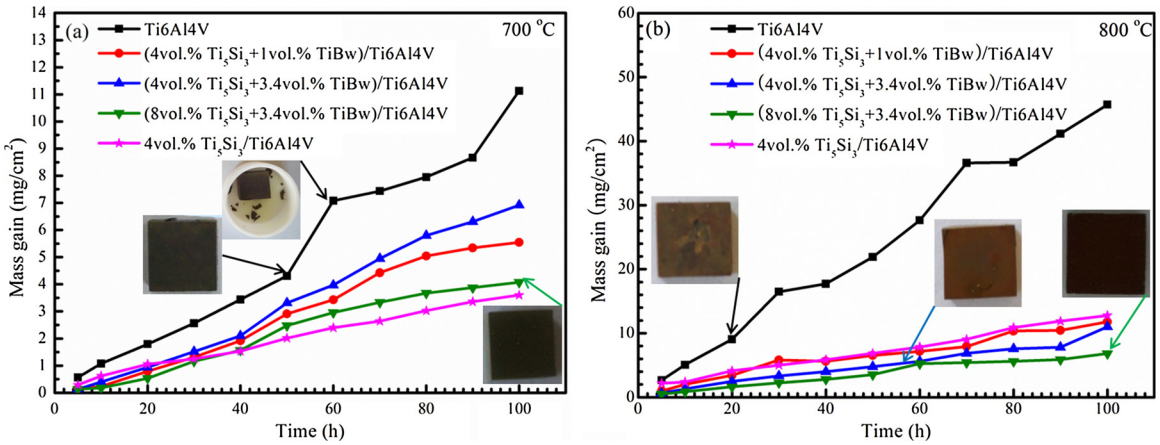

Fig. 3. Mass gain-time curves of Ti6Al4V alloys, 4 vol.%Ti_5Si_3/Ti6Al4V composites and (Ti_5Si_3 + TiBw)/Ti6Al4V composites with different reinforcements fractions after oxidizing at 700 °C (a) and 800 °C (b).

can be found that the ΔG value of each reaction is negative, which indicates that the four reactions can take place thermodynamically. In addition, Al element is most likely to react with O element. Compared with the TiBw and Ti_5Si_3 reinforcements, the Ti6Al4V matrix alloy tends to oxidize preferentially. Previous studies reported that the oxidation products of TiB are TiO_2 and B_2O_3, respectively [23]. However, B_2O_3 can evaporate above 750 °C [23]. As reported, the oxidation process of Ti-Si-B was accompanied with outward diffusion of B in the form of volatile B_2O_3 at 500 °C [24]. According to Vojtěch et al. [15], the oxidation products of Ti_5Si_3 are TiO_2 and SiO_2, respectively. Ti_5Si_3 possesses excellent oxidation resistance below 850 °C [16].

3.2. Oxidation mass-gain analysis

Fig. 3 presents curves of the weight gain per unit surface area versus the oxidation time for Ti6Al4V alloys, 4 vol.%Ti_5Si_3/Ti6Al4V composites and (Ti_5Si_3 + TiBw)/Ti6Al4V composites with different reinforcements fractions after oxidizing at 700 and 800 °C. Overall, the mass gain of Ti_5Si_3/Ti6Al4V and (Ti_5Si_3 + TiBw)/Ti6Al4V composites is lower than that of Ti6Al4V alloys at both temperatures. Firstly, the Ti_5Si_3/Ti6Al4V composite and (Ti_5Si_3 + TiBw)/Ti6Al4V composites with different fractions show similar oxidation weight gain at 700 °C for 40 h. After oxidation for 50 h, the Ti_5Si_3/Ti6Al4V composite exhibits the lowest oxidation rate, which may be due to two aspects, 1) more and finer Ti_5Si_3 particles in the matrix. The SiO_2 scale formed by Ti_5Si_3 layer could further suppress the oxidation of TiAl alloy [25]; 2) the absence of TiBw reinforcement in the Ti_5Si_3/Ti6Al4V composite. According to Hu et al. [6], TiBw could bring in more boundaries and decrease oxidation resistance of composites. Moreover, the mass gain increases with increasing the content of TiBw. These results demonstrate that Ti_5Si_3 particles play a more important role in improving oxidation resistance of the composites at 700 °C, compared with TiB whiskers. Secondly, after the composites were oxidized at 800 °C, the mass gain reduces with the increase in Ti_5Si_3 fractions. As reported [26], the oxidation resistance of TiAlSiZr alloys is better than that of TiAlSi alloys, owing to the increased silicides in Ti matrix. However, the oxidation resistance of Ti_5Si_3/Ti6Al4V composite at 800 °C became lower than that of the composites with different TiBw fractions. This is may be attributed to the microstructure of Ti_5Si_3/Ti6Al4V composite, which is similar to the coarse Widmanstätten microstructure of Ti6Al4V matrix. At the early stage of oxidation process, the growth rate of oxide scale could be decreased by fine grains, which could induce more short-circuit diffusion paths [27]. Besides, fine Ti_5Si_3 particles merely distributing in the β-Ti phases plays a limited role in improving oxidation resistance. In the Ti6Al4V matrix, the fraction of α-Ti is greater than β-Ti. The high-solubility of oxygen in α-Ti (approximately 30 at.% at 700 °C [28]) resulted in the growth of oxides on metal surfaces, and the permeation of oxygen from surface into substrate during oxidation process. It is worth noting that the mass gain decreases with increasing TiBw fractions. This phenomenon may be caused by the formation and evaporation of B_2O_3 at 800 °C, as reported by Hu et al. [6]. Lastly, the mass gain of all specimens increases with increasing oxidation temperatures. The (8 vol.%Ti_5Si_3 + 3.4 vol.%TiBw)/Ti6Al4V composite shows superior oxidation resistance at 700 and 800 °C, compared with the Ti6Al4V alloy and the composites with 4 vol.%Ti_5Si_3 reinforcement. Ti_5Si_3 particles and TiB whiskers distributing around the Ti6Al4V particles can suppress oxygen diffusion. The effects of the reinforcements are similar to that of TiCp wall during the oxidation process of TiCp/Ti6Al4V composites [29]. Compared with the as-sintered Ti6Al4V alloy, the matrix microstructure of composites was refined by TiBw and Ti_5Si_3 reinforcements inhibiting the growth of α phases (as shown in Fig. 1).

Additionally, the macro surface images of oxidized samples for different times are presented in Fig. 3. The images clearly reveal the improvement in oxidation resistance of (Ti_5Si_3 + TiBw)/Ti6Al4V composites, compared with the Ti6Al4V alloys. After oxidizing at 700 °C for 50 h and 800 °C for 20 h, spallation of oxide scale is evident in Ti6Al4V alloys, which is due to the internal stresses caused by a distortion of crystal lattice via oxygen diffusing into Ti matrix. Noticeable oxide scale spallation can be found in the (4 vol.%Ti_5Si_3 + 3.4 vol.%TiBw)/Ti6Al4V composite at 800 °C for 60 h. However, the surfaces of (8 vol.%Ti_5Si_3 + 3.4 vol.%TiBw)/Ti6Al4V composites remain relatively flat, and no oxidation spallation can be observed at 700 and 800 °C for 100 h. This phenomenon distinctly demonstrates that the addition of Ti_5Si_3 reinforcements significantly improves the adherence and impedes the spallation of oxide scale in the composites.

3.3. Phase identification

Fig. 4 shows XRD patterns for Ti6Al4V alloy, 4 vol.%Ti_5Si_3/Ti6Al4V composite, and (Ti_5Si_3 + TiBw)/Ti6Al4V composites with different reinforcements fractions after oxidation tests at 700 °C for 100 h. Rutile TiO_2 phase is the dominant oxidation product, due to high Ti content in the composites. The diffusion rate of Al in Al_2O_3 is slower than that of Ti in TiO_2, thus, the formation of Al_2O_3 scale were suppressed by TiO_2 scale in the single Ti6Al4V system. However, a small number of Al_2O_3 and SiO_2 phases were detected in the composites including nano-Ti_5Si_3 particles. It is well known that continuous and dense Al_2O_3 and SiO_2 scales are beneficial to improving oxidation resistance [16].

Fig. 5 exhibits XRD results for oxidized (8 vol.%Ti_5Si_3 + 3.4 vol.%TiBw)/Ti6Al4V composites at different temperatures and time periods. The oxidation products include rutile TiO_2, Al_2O_3 and SiO_2 phases

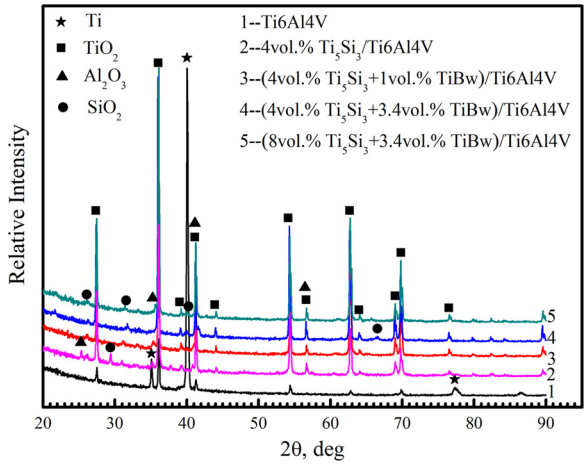

Fig. 4. X-ray diffraction patterns for Ti6Al4V alloy, 4 vol.%Ti_5Si_3/Ti6Al4V composite and (Ti_5Si_3 + TiBw)/Ti6Al4V composites with different reinforcements fractions after oxidation tests at 700 °C for 100 h.

at 700 and 800 °C. Among TiO_2, rutile and anatase are the most common phases. The transition from anatase to rutile phase is irreversible at about 700 °C [1]. B_2O_3 was not observed in the XRD results, which is probably due to evaporation [6]. Compared with the oxidation products at 700 °C, the fractions of Al_2O_3 and SiO_2 phases increase at 800 °C. Therefore, the oxidation resistance of composites was improved by a large margin, compared with the Ti6Al4V alloy at 800 °C (Fig. 3(b)). Similar results are observed in Fig. 5(b). The fractions of Al_2O_3 and SiO_2 phases increase with increasing oxidation time. These results also indicate that nano-Ti_5Si_3 can increase the formation rate of dense Al_2O_3 and SiO_2 scales.

The oxidation process of Ti is complex, due to the existence of several stable oxides in Ti-O system, such as TiO, Ti_2O and Ti_3O. According to Ti-O diagram [30], TiO_2 is the main oxidation product under the conditions of atmospheric oxygen partial pressure and 1000 °C. TiO_2 scale is non-protective, due to the high solid solubility of oxygen in titanium, and more defects in the transition region. Ti alloys have lower oxidation resistance, owing to the formation of polyporous TiO_2 scale or $TiO_2 + Al_2O_3$ mixed scale [31]. Thermodynamically, α-Al_2O_3 is one of the most stable oxides among the oxidation products of Al. Due to the low diffusion rate of oxygen in Al_2O_3 as well as the continuous and dense microstructure, the Al_2O_3 scale can protect Ti alloys from oxidation. It was reported that the oxidation rate of Ti alloys can be decreased by a continuous SiO_2 scale [32].

It can be seen from Figs. 4 and 5 that the oxidation products are TiO_2, Al_2O_3 and SiO_2. Under high temperatures, unstable B_2O_3 formed a vitreous layer or evaporated, which resulted in the depletion of B and the formation of TiO_2 scale with pores [24]. Compared with the unstable B_2O_3, SiO_2 possesses high viscosity and low vapor pressure, which is beneficial to improving oxidation resistance [24].

3.4. Morphology of oxide scale

Fig. 6 reveals SEM micrographs of the cross-section of the oxidized samples at 700 °C for 100 h. Thick and layered oxide scale with spallation are observed in Fig. 6(a). Cracks and pores present at the oxide/alloys interface. The reason of the cracks and spallation in oxide scale is the brittleness of porous scale as well as thermal and growing stresses during the high-temperature oxidation process. Yu et al. [33] reported that the oxidation rate at 700 °C after 20 h is increased by the failure of oxide scale. According to Du et al. [34], due to alternate growth of Al_2O_3 and TiO_2 layers by outward diffusion of Al and inward diffusion of O, a multilayered oxide scale formed on the surface of Ti6Al4V alloy. Once the thickness of oxide scale exceeded critical value, cracks presented at the matrix/scale interface and interface bonding weakened.

In contrast, as seen in Fig. 6(b)-(e), the oxide scales of the composites including nano-Ti_5Si_3 are relatively thin and dense, and no spallation is observed. This result verifies that the oxidation resistance of composites is better than that of Ti6Al4V alloy. Nano-Ti_5Si_3 is beneficial to decreasing the oxidation rate of composites. As a previous study showed [35], a combination effect of matrix and Ti_5Si_3 phase enhanced the oxidation resistance of Ti_3Al alloys with Si addition. Moreover, with increasing the content of Si, the oxidation resistance of Ti_3Al alloys was increased at 800 °C. It is well known that a well adhered oxide scale can decrease oxidation rate effectively. For the oxidized Ti6Al4V alloy at 700 °C, the adhesion of oxide scale is weak and separated from the substrate. Coddet et al. [36] claimed that the adhesion strength of oxide scale in Ti alloys tends to be zero at 700 °C. However, the oxide scales of (Ti_5Si_3 + TiBw)/Ti6Al4V composites exhibit excellent spallation resistance at 700 °C for 100 h. Furthermore, it can be found from Fig. 6(f) that reinforcements pin oxide scale and improve interface adhesion. The aforementioned analysis of cross-section morphology demonstrates that the addition of Ti_5Si_3 reinforcement drastically enhances the oxidation resistance of Ti6Al4V alloy. The Ti_5Si_3 and TiBw reinforcements can fasten oxide scale effectively. Dai et al. [37] adopted first principles calculations and proved that Si can partially improve the adhesion between TiO_2 and TiAl substrate. In addition, reinforcements can release the growth and thermal stresses generated during oxidation process.

SEM and TEM micrographs of oxide scales on Ti6Al4V alloy and (Ti_5Si_3 + 3.4 vol.%TiBw)/Ti6Al4V composites with different Ti_5Si_3

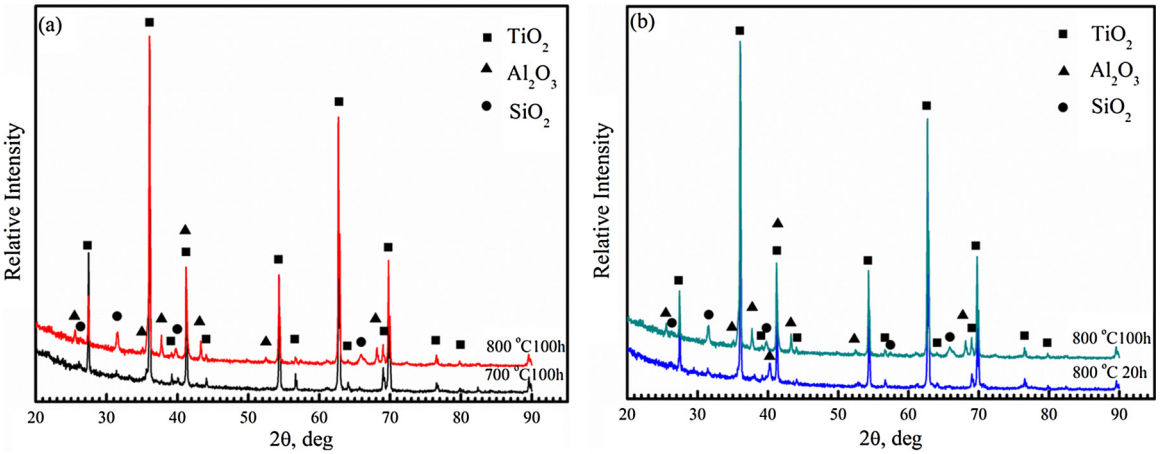

Fig. 5. X-ray diffraction patterns for oxidized (8 vol.%Ti_5Si_3 + 3.4 vol.%TiBw)/Ti6Al4V composites at different temperatures for 100 h (a) and at 800 °C for different time periods (b).

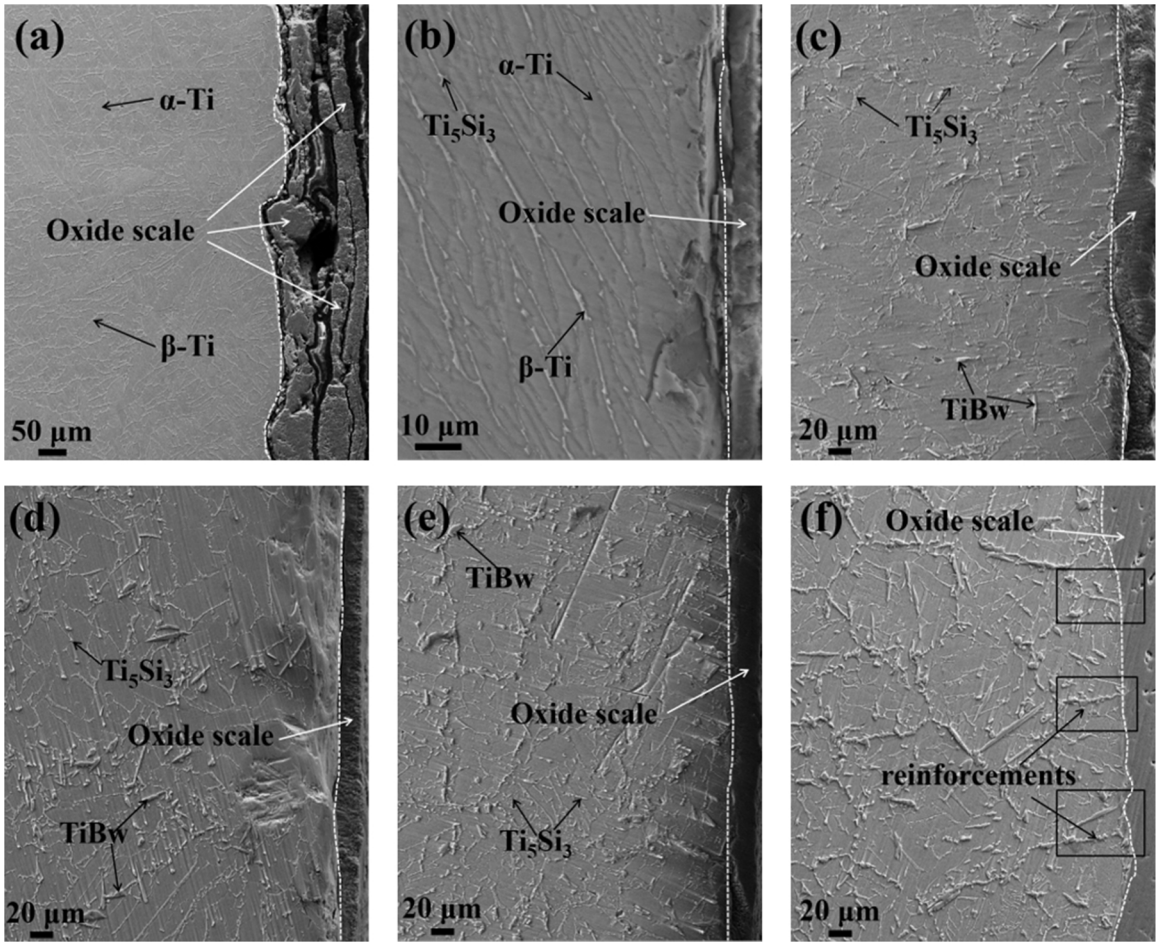

Fig. 6. SEM micrographs of cross-section of Ti6Al4V alloy (a), 4 vol.%Ti_5Si_3/Ti6Al4V composite (b), (4 vol.%Ti_5Si_3 + 1 vol.%TiBw) composite (c), (4 vol.%Ti_5Si_3 + 3.4 vol.%TiBw) composite (d), (8 vol.%Ti_5Si_3 + 3.4 vol.%TiBw) composite (e) and (f) after oxidation tests at 700 °C for 100 h.

fractions are shown in Fig. 7. In addition, the EDS results of the oxidation products in composites are exhibited in Fig. 7(b) and (d). According to XRD and EDS results, the oxide with cylindrical shape is rutile TiO_2, and the approximately equiaxed oxide is Al_2O_3. The result is consistent with that in our previous studies [29]. As shown in Fig. 7(a), the size of rutile TiO_2 particles in the Ti6Al4V alloy is larger than that in the composites (Fig. 7(b) and (c)). Introducing nano-Ti_5Si_3 particles refined the TiO_2 particles and reduced the size of α phases, which is beneficial to forming a compact oxide scale. This result is in agreement with the previous investigation: Si element promoted the formation of a dense TiO_2 layer [17].

Fig. 8 presents SEM morphologies of the oxidized surfaces of Ti6Al4V alloy, 4 vol.%Ti_5Si_3/Ti6Al4V composite and (Ti_5Si_3 + TiBw)/Ti6Al4V composites with different fractions at 800 °C for 100 h. It is obvious that oxide scales of the Ti6Al4V alloy (Fig. 8(a)) and composites with 4 vol.%Ti_5Si_3 reinforcement exhibit spallation and cracks (Fig. 8(c), (d) and (e)). For alloy and composites, the sub-surface were oxidized constantly, after the spallation of surface (Fig. 8(a) and (c)). By comparing Fig. 8(d) and 8(e), it is recognized that the surface spallation becomes more serious with increasing the TiBw fractions from 1 vol.% to 3.4 vol.%. However, the surface morphology of (8 vol.%Ti_5Si_3 + 3.4 vol.%TiBw)/Ti6Al4V composite is smooth and flat, besides the crack presents at the corner of the specimen, as seen in Fig. 8(f). This phenomenon suggests that the oxidation extent of Ti6Al4V alloy and composites with 4 vol.%Ti_5Si_3 reinforcements is more serious than that of (8 vol.%Ti_5Si_3 + 3.4 vol.%TiBw)/Ti6Al4V composite. The oxidation resistance of composites improves with increasing Ti_5Si_3 fractions. Compared with the (4 vol.%Ti_5Si_3 + 3.4 vol.%TiBw)/Ti6Al4V composite, more and connected Ti_5Si_3 particles distribute around the matrix in the composite with 8 vol.%Ti_5Si_3 reinforcement. Ti_5Si_3 particles can decrease the oxidation rate of Ti-Si alloys [13]. Additionally, through comparing the high magnified SEM morphologies of oxide scales (Fig. 8(b) and 8(g)), it can be seen that the particle size of oxide in composites was refined by the addition of reinforcements.

The TiBw reinforcement cannot be easily observed, as shown in Fig. 8(d), (e) and (f). This phenomenon is due to the oxidation of TiB phase and the evaporation of B_2O_3 at 800 °C, as reported by Lee et al. [38]. In addition, the channels within oxide scale formed by B_2O_3 can accelerate the inward diffusion of oxygen. This confirms that increasing fractions of TiBw results in more serious oxidation of composites at higher temperature. Besides, Qin et al. [39] also deduced that TiB transfer into amorphous boron oxide partially at 700 °C. Therefore, the weight gain versus time plots (Fig. 3(b)) cannot estimate the true oxidation behavior at 800 °C, owing to the weight loss caused by TiB reinforcement. From the above analysis, it can be concluded that the oxidation resistance increases with increasing Ti_5Si_3 fractions, however, decreases with increasing TiBw fractions.

3.5. Anti-oxidation mechanisms

In order to further elucidate the anti-oxidation mechanisms of titanium matrix composites, the microstructure of cross-section and corresponding EDS results, as well as the elemental line and surface scanning results of the oxidized (8 vol.%Ti_5Si_3 + 3.4 vol.%TiBw)/Ti6Al4V composite at 800 °C for 100 h are shown in Fig. 9. On the basis

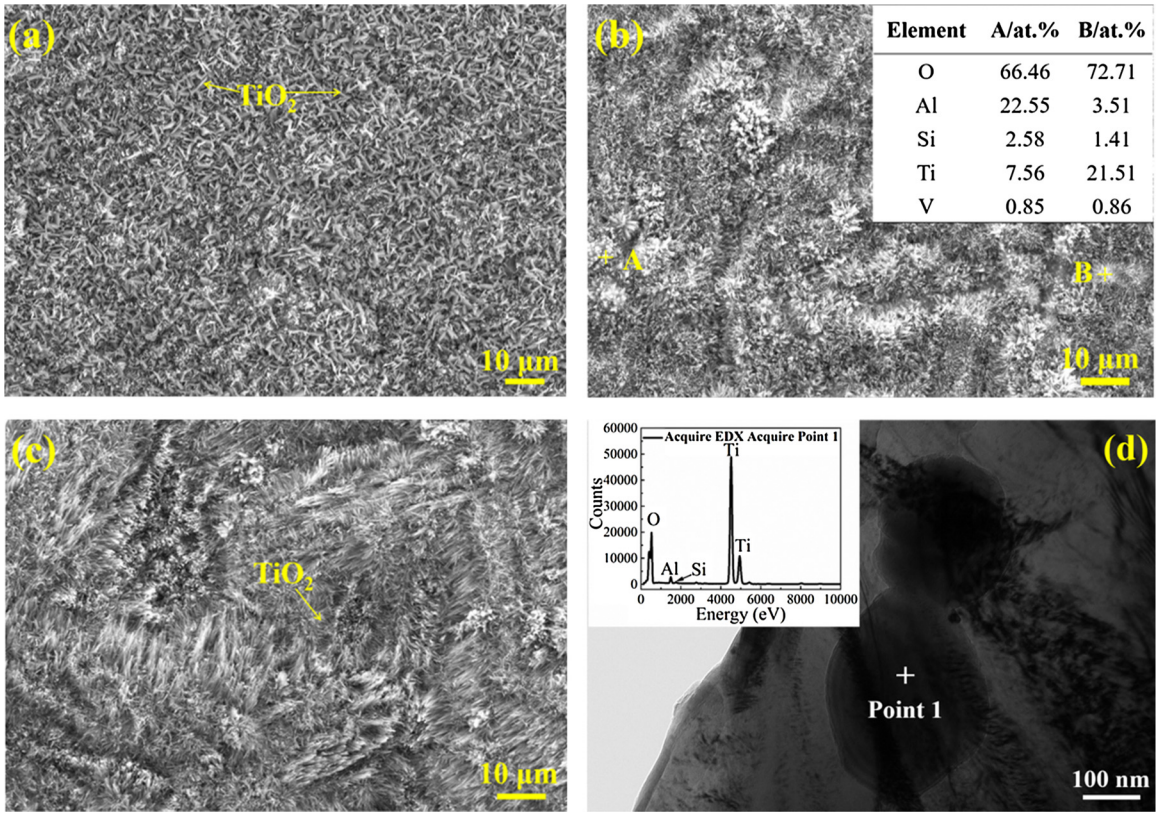

Fig. 7. SEM micrographs of oxide scales on Ti6Al4V alloy (a), (8 vol.%Ti_5Si_3 + 3.4 vol.%TiBw) composite (b); SEM and TEM micrographs of oxide scale on (4 vol.%Ti_5Si_3 + 3.4 vol.%TiBw) composite (c) and (d) at 700 °C for 100 h.

of the EDS and scanning results (Fig. 9(a), (b) and (c)), the oxide scale of composite can be roughly divided into two layers. Combining with the XRD results in Fig. 4, it is identified that Al_2O_3 and SiO_2 are the dominant phases in the outer layer, while TiO_2 is the primary phase in the inner layer. The formation of SiO_2 in oxide scale is related to Ti_5Si_3 phase. The reasons for the formation of thin Al_2O_3 and SiO_2 mixed layer are as follows. Firstly, TiO_2 with faster growth rate restrained the formation of Al_2O_3. Secondly, the content of Al and Si within the composite is limited. In the Ti alloys, the maximum content of aluminum is 6 wt.% [1]. However, it was reported that in TiAl alloys, the content of Al for forming a protective scale is about 57–59 at.% [6]. For forming a protective SiO_2 scale, the concentration of Si must exceed 40 at.% [40]. The high concentration of Si or Al in Ti alloys can deteriorate mechanical properties, such as high-temperature strength and room-temperature ductility [41].

The formation of the layered oxide scales are attributed to the following aspects. At the early stage of oxidation process, TiO_2 formed on the substrate initially, as proved in the previous investigations [34]. Afterwards, the partial pressure of oxygen at the TiO_2/substrate interface decreased, then Al_2O_3 and SiO_2 occupied the external air/oxide interface. Using the data in Gale et al. [42], the diffusion coefficients (D) of Al and Si in α-Ti were calculated, and the results exhibit the D

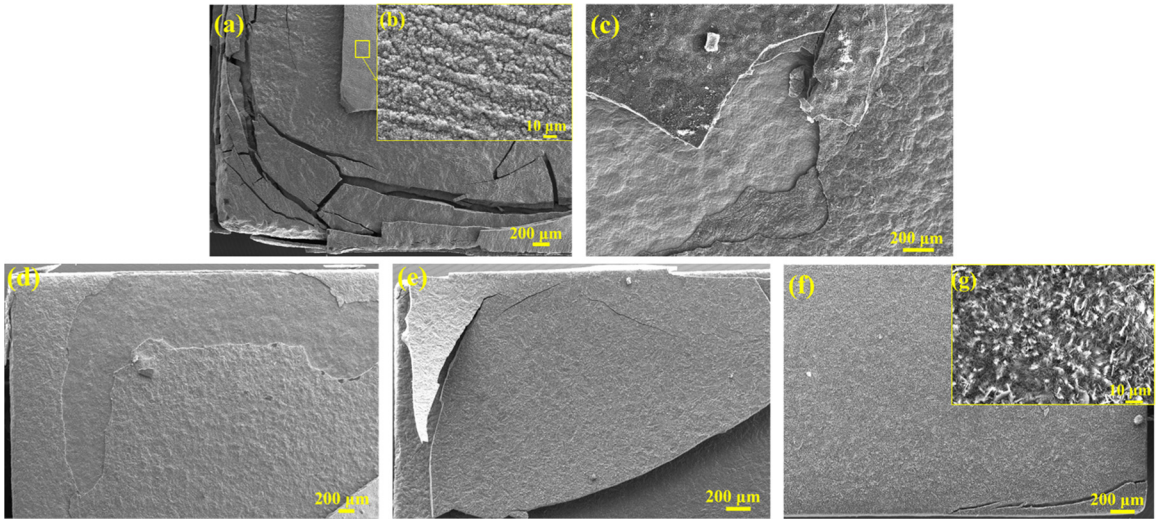

Fig. 8. SEM morphologies of oxidized surfaces of Ti6Al4V alloy (a) and (b), 4 vol.%Ti_5Si_3/Ti6Al4V composite (c) (4 vol.%Ti_5Si_3 + 1 vol.%TiBw) composite (d), (4 vol.%Ti_5Si_3 + 3.4 vol.%TiBw) composite (e), (8 vol.%Ti_5Si_3 + 3.4 vol.%TiBw) composite (f) and (g) at 800 °C for 100 h.

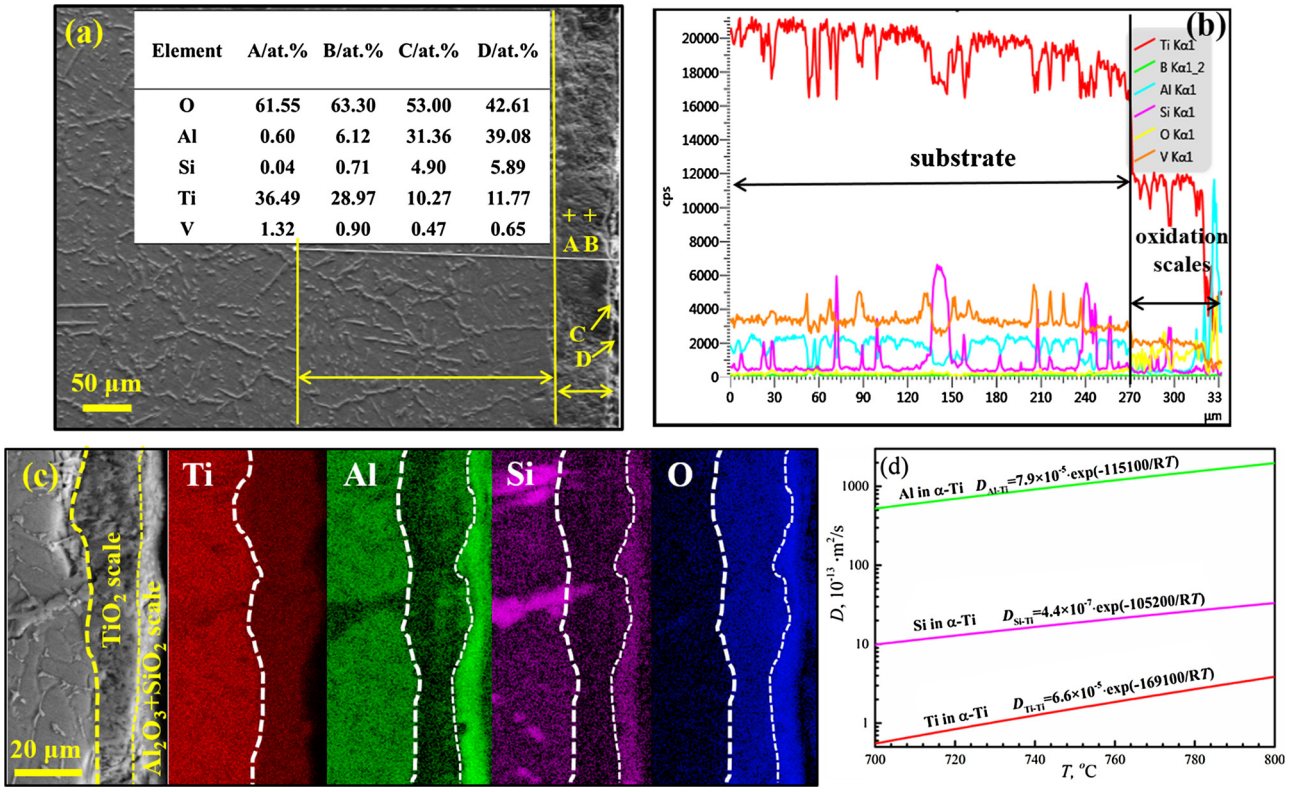

Fig. 9. Cross-sectional SEM micrographs (a), elemental line scanning (b) and surface scanning results (c) of oxidized (8 vol.%Ti_5Si_3 + 3.4 vol.%TiBw)/Ti6Al4V composite at 800 °C for 100 h; the diffusion coefficient for Al, Si and Ti in α-Ti from 700 to 800 °C (d).

value of Ti self-diffusion is lower, as shown in Fig. 9(d). The outer Al_2O_3 and SiO_2 layer were formed by outward diffusion of Al and Si with continuous oxidation process. The inner TiO_2 scale grew through oxygen diffusing into substrate, as reported by Hu et al. [6]. The polyporous TiO_2 scale provides diffusion channel for oxygen, however, the mixed outer oxide scale of Al_2O_3 and SiO_2 provides diffusion obstacles for oxygen. Therefore, the Al_2O_3 and SiO_2 scale can alleviate oxidation progress of composite.

In addition, as shown in Fig. 9(b) and (c), a small quantity of Al_2O_3 and SiO_2 presenting in the TiO_2 scale were detected. In previous studies of Ti-Si alloys [15], the oxidation of silicide generated SiO_2 particles, which were detected in oxide scale. This phenomenon was caused by the silicide particles in matrix dissolved into the TiO_2 scale [15]. In the composite, the SiO_2 particles changed the stress-relaxation process, and facilitated the formation of a more dense TiO_2 scale with fewer defects and lower porosity, therefore, the oxidation resistance of composite was improved. Additionally, Ti_5Si_3 particles distributing at grain boundaries and phase interfaces can act as diffusion barriers and decrease diffusion rate of O into matrix. Ti_5Si_3 particles fastened the TiO_2 scale and enhanced the interface adhesion.

4. Conclusions

(1) Nano-Ti_5Si_3 particles can significantly improve oxidation resistance of titanium matrix.
(2) After oxidized at 800 °C for 100 h, the weight gain of (8 vol.%Ti_5Si_3 + 3.4 vol.%TiBw)/Ti6Al4V composite accounted for 15% of the Ti6Al4V alloy. The oxide scale of Ti6Al4V alloy exhibited spallation and cracks. However, the oxide scale of (8 vol.%Ti_5Si_3 + 3.4 vol.%TiBw)/Ti6Al4V composite remained flat without spallation.
(3) The oxidation rate of composites decreased with increasing Ti_5Si_3 fractions, but increased with increasing TiBw fractions. Refining TiO_2 particles and increasing Al_2O_3 and SiO_2 fractions by nano-Ti_5Si_3 particles are beneficial to forming dense oxide scale.
(4) The refinement of TiO_2 particles, thin and protective Al_2O_3 and SiO_2 mixed scale as well as oxide scale fastened by reinforcements result in the prominent enhancement in oxidation resistance of (Ti_5Si_3 + TiBw)/Ti6Al4V composites.

Acknowledgements

This work is financially supported by the National Key R&D Program of China (No. 2017YFB0703100), the National Natural Science Foundation of China (NSFC) under Grant Nos. 51671068, 51731009 and 51471063. Y. Jiao would like to acknowledge China Scholarship Council (Grant No. 201606120109) for supporting her one year exchange (2016.9-2017.9) in McGill University, Canada.

References

[1] H. Guleryuz, H. Cimenoglu, Oxidation of Ti-6Al-4V alloy, J. Alloy Compd. 472 (2009) 241–246.
[2] P.A.J. Bagot, A. Radecka, A.P. Magyar, Y. Gong, D.C. Bell, G.D.W. Smith, M.P. Moody, D. Dye, D. Rugg, The effect of oxidation on the subsurface microstructure of a Ti-6Al-4V alloy, Scripta Mater. 148 (2018) 24–28.
[3] D.A. Brice, P. Samimi, I. Ghamarian, Y. Liu, R.M. Brice, R.F. Reidy, J.D. Cotton, M.J. Kaufman, P.C. Collins, Oxidation behavior and microstructural decomposition of Ti-6Al-4V and Ti-6Al-4V-1B sheet, Corros. Sci. 112 (2016) 338–346.
[4] J.H. Luan, Z.B. Jiao, G. Chen, C.T. Liu, Improved ductility and oxidation resistance of cast Ti-6Al-4V alloys by microalloying, J. Alloy Compd. 602 (2014) 235–240.
[5] L.J. Huang, L. Geng, H.X. Peng, Microstructurally inhomogeneous composites: Is a homogeneous reinforcement distribution optimal? Prog. Mater. Sci. 71 (2015) 93–168.
[6] H. Hu, L. Huang, L. Geng, B. Liu, B. Wang, Oxidation behavior of TiB-whisker-reinforced Ti60 alloy composites with three-dimensional network architecture, Corros. Sci. 85 (2014) 7–14.
[7] S. Wang, L.J. Huang, L. Geng, F. Scarpa, Y. Jiao, H.X. Peng, Significantly enhanced creep resistance of low volume fraction in-situ TiBw/Ti6Al4V composites by architectured network reinforcements, Sci. Rep. 7 (2017) 40823.
[8] S.L. Wei, L.J. Huang, X.T. Li, Q. An, L. Geng, Interactive effects of cyclic oxidation and structural evolution for Ti-6Al-4V/(TiC + TiB) alloy composites at elevated temperatures, J. Alloy Compd. 752 (2018) 164–178.

[9] S.C. Tjong, Y.-W. Mai, Processing-structure-property aspects of particulate- and whisker-reinforced titanium matrix composites, Compos. Sci. Technol. 68 (2008) 583–601.
[10] Y. Jiao, L.J. Huang, S. Wang, X.T. Li, Q. An, X.P. Cui, L. Geng, Effects of first-scale TiBw on secondary-scale Ti_5Si_3 characteristics and mechanical properties of in-situ (Ti_5Si_3 + TiBw)/Ti6Al4V composites, J. Alloy Compd. 704 (2017) 269–281.
[11] E. Zhang, G. Zeng, S. Zeng, Effect of in situ TiB short fibre on oxidation behavior of Ti-6Al-1.2B alloy, Scripta Mater. 46 (2002) 811–816.
[12] Z. Tang, J.J. Williams, A.J. Thom, M. Akinc, High temperature oxidation behavior of Ti_5Si_3-based intermetallics, Intermetallics 16 (2008) 1118–1124.
[13] D. Vojtěch, B. Bártová, T. Kubatík, High temperature oxidation of titanium-silicon alloys, Mater. Sci. Eng. A 361 (2003) 50–57.
[14] H.-R. Jiang, Z.-L. Wang, W.-S. Ma, X.-R. Feng, Z.-Q. Dong, L. Zhang, Y. Liu, Effects of Nb and Si on high temperature oxidation of TiAl, T Nonferr. Metal. Soc. 18 (2008) 512–517.
[15] D. Vojtěch, H. Čížová, K. Jurek, J. Maixner, Influence of silicon on high-temperature cyclic oxidation behaviour of titanium, J. Alloy Compd. 394 (2005) 240–249.
[16] W. Zhou, Y.G. Zhao, W. Li, Q.D. Qin, B. Tian, S.W. Hu, Al-Si coating fused by Al + Si powders formed on Ti-6Al-4V alloy and its oxidation resistance, Mater. Sci. Eng. A 430 (2006) 142–150.
[17] L. Shi-Yu, S. Jia-Xiang, W. Fu-He, Z. Yue, Surface segregation of Si and its effect on oxygen adsorption on a γ-TiAl(111) surface from first principles, J. Phys. Condens. Matter 21 (2009) 225005.
[18] J. Zhu, A. Kamiya, T. Yamada, A. Watazu, W. Shi, K. Naganuma, Effect of silicon addition on microstructure and mechanical properties of cast titanium alloys, Mater. Trans 42 (2001) 336–341.
[19] S. Shu, B. Xing, F. Qiu, S. Jin, Q. Jiang, Comparative study of the compression properties of TiAl matrix composites reinforced with nano-TiB_2 and nano-Ti_5Si_3 particles, Mater. Sci. Eng. A 560 (2013) 596–600.
[20] Y. Jiao, L.J. Huang, T.B. Duan, S.L. Wei, B. Kaveendran, L. Geng, Controllable two-scale network architecture and enhanced mechanical properties of (Ti_5Si_3 + TiBw)/Ti6Al4V composites, Sci. Rep.-UK 6 (2016).
[21] Y. Jiao, L.J. Huang, Q. An, S. Jiang, Y.N. Gao, X.P. Cui, L. Geng, Effects of Ti_5Si_3 characteristics adjustment on microstructure and tensile properties of in-situ (Ti_5Si_3 + TiBw)/Ti6Al4V composites with two-scale network architecture, Mater. Sci. Eng. A 673 (2016) 595–605.
[22] Y. Liang, Y. Che, Handbook of Thermodynamic Data for Inorganic Substances, Northeastern University, Shenyang, 1993.
[23] E. Zhang, G. Zeng, S. Zeng, Oxidation behavior of in situ TiB short fibre reinforced Ti-6Al-1.2B alloy in air, J. Mater. Sci. 37 (2002) 4063–4071.
[24] B. Grančič, M. Mikula, T. Roch, P. Zeman, L. Satrapinskyy, M. Gregor, T. Plecenik, E. Dobročka, Z. Hájovská, M. Mičušík, A. Šatka, M. Zahoran, A. Plecenik, P. Kúš, Effect of Si addition on mechanical properties and high temperature oxidation resistance of Ti-B-Si hard coatings, Surf. Coat. Technol. 240 (2014) 48–54.
[25] X.Y. Li, S. Taniguchi, Y. Matsunaga, K. Nakagawa, K. Fujita, Influence of siliconizing on the oxidation behavior of a γ-TiAl based alloy, Intermetallics 11 (2003) 143–150.
[26] S. Tkachenko, O. Datskevich, K. Dvořák, Z. Spotz, L. Kulak, L. Čelko, Isothermal oxidation behavior of experimental Ti-Al-Si alloys at 700 °C in air, J. Alloy Compd. 694 (2017) 1098–1108.
[27] J. He, Y. Luan, H. Guo, H. Peng, Y. Zhang, T. Zhang, S. Gong, The role of Cr and Si in affecting high-temperature oxidation behaviour of minor Dy doped NiAl alloys, Corros. Sci. 77 (2013) 322–333.
[28] T. Kitashima, L.J. Liu, H. Murakami, Numerical analysis of oxygen transport in alpha titanium during isothermal oxidation, J. Electrochem. Soc. 160 (2013) 441–444.
[29] L.J. Huang, L. Geng, Y. Fu, B. Kaveendran, H.X. Peng, Oxidation behavior of in situ TiCp/Ti6Al4V composite with self-assembled network microstructure fabricated by reaction hot pressing, Corros. Sci. 69 (2013) 175–180.
[30] M.H.S. Nagasaki, Binary Alloy Phase-Diagrams Book, Metallurgical Industry Press, Beijing, 2003, p. 320.
[31] T. Kitashima, T. Kawamura, Prediction of oxidation behavior of near-α titanium alloys, Scripta Mater. 124 (2016) 56–58.
[32] C. Chen, X. Feng, Y. Shen, Oxidation behavior of a high Si content Al-Si composite coating fabricated on Ti-6Al-4V substrate by mechanical alloying method, J. Alloy Compd. 701 (2017) 27–36.
[33] C. Yu, S. Zhu, D. Wei, F. Wang, Oxidation and H_2O/NaCl-induced corrosion behavior of sputtered Ni-Si coatings on Ti6Al4V at 600-650 °C, Surf. Coat. Technol. 201 (2007) 7530–7537.
[34] H.L. Du, P.K. Datta, D.B. Lewis, J.S. Burnell-Gray, Air oxidation behaviour of Ti-6Al-4V alloy between 650 and 850 °, Corros. Sci. 36 (1994) 631–642.
[35] J.S. Wu, L.T. Zhang, F. Wang, K. Jiang, G.H. Qiu, The individual effects of niobium and silicon on the oxidation behaviour of Ti_3Al based alloys, Intermetallics 8 (2000) 19–28.
[36] C. Coddet, A.M. Craze, G. Beranger, Measurements of the adhesion of thermal oxide films: application to the oxidation of titanium, J. Mater. Sci. 22 (1987) 2969–2974.
[37] J.H. Dai, Y. Song, R. Yang, Influence of alloying elements on stability and adhesion ability of TiAl/TiO_2 interface by first-principles calculations, Intermetallics 85 (2017) 80–89.
[38] D.B. Lee, Y.C. Lee, D.J. Kim, The oxidation of TiB_2 ceramics containing Cr and Fe, Oxid. Met. 56 (2001) 177–189.
[39] Y. Qin, D. Zhang, W. Lu, J. Qin, D. Xu, Oxidation behavior of in situ synthesized TiB/Ti-Al composite, J. Mater. Sci 40 (2005) 6553–6558.
[40] B.V. Cockeram, R.A. Rapp, Oxidation-resistant boron- and germanium-doped silicide coatings for refractory metals at high temperature, Mater. Sci. Eng. A 192 (1995) 980–986.
[41] Z.D. Xiang, S.R. Rose, P.K. Datta, Codeposition of Al and Si to form oxidation-resistant coatings on γ-TiAl by the pack cementation process, Mater. Chem. Phys. 80 (2003) 482–489.
[42] W.F. Gale, T.C. Totemeier, Smithells Metals Reference Book, Butterworth-Heinemann (2003).